Transactions, SMiRT-24
BEXCO, Busan, Korea - August 20-25, 2017
Division II

Unstable Fracture Assessment of Weldments of Weldolets using CDFD Method based on Elastic-Plastic Finite Element Analyses

Tae-Jin Kim[1], Jae-Min Gim[2], Kyung-dong Bae[2], Se-Chang Kim[3], Nam-Su Huh[4], Yun-Jae Kim[5] and Jun-Seog Yang[6]

[1] Graduate Student, Department of Mechanical System Design Engineering, Seoul Nat'l Univ. of Science and Technology, Korea
[2] Graduate Student, Mechanical Engineering, Korea Univ., Korea
[3] Postdoctoral Researcher, Mechanical Engineering, Sungkyunkwan Univ., Korea
[4] Professor, Department of Mechanical System Design Engineering, Seoul Nat'l Univ. of Science and Technology, Korea
[5] Professor, Mechanical Engineering, Korea University, Korea
[6] Korea Hydro & Nuclear Power Co., Ltd, Korea

ABSTRACT

To apply break exclusion criteria to nuclear high-energy piping systems, a 100% volumetric inspection of all pipe welds should be conducted. However, fracture mechanics assessment is required as an alternative requirement to ensure the safety of the welds if in-service inspection with 100% coverage is not attained. In this study, the critical crack lengths were computed for the circumferential through-wall cracks (TWCs) in weldolet weldments of T-branches based on the crack driving force diagram (CDFD) method. In terms of crack locations, the cracks were postulated on the upper fusion line. The applied *J*-integral curves were obtained as calculating the *J* values for several crack lengths using elastic-plastic finite element (FE) analysis. Consequently, the critical crack lengths (CCLs) for faulted conditions were determined by comparing the material resistance *J-R* curve with the applied *J*-integral curve.

INTRODUCTION

Supplementary structures such as pipe whip restraints and jet impingement shields are installed to minimize the dynamic effects of a postulated pipe rupture in nuclear high-energy piping systems (KINS 2014, USNRC 2016), even though the additional constructions cause costs and unexpected loadings due to excessive constraints. However, the installation of the structures can be reduced if the break exclusion concept is applicable to the piping systems.

The break exclusion criteria requires a 100% volumetric examination by augmented in-service inspection of all pipe welds (KINS 2014, USNRC 2017). Nevertheless, the 100% volumetric inspection is impossible for some welds due to limitation of the on-site inspection and structural complexity. For the application of the break exclusion criteria to uninspected welds, fracture mechanics assessment is required as an alternative to demonstrate that the probability of a pipe break is sufficiently low during plant operation. As an example of the alternative qualification, Virginia Electric and Power Company (2005, 2006) carried out the integrity assessment of a postulated crack in branch connection weldolets and heat exchangers in Surry power station unit 2 for relief requests of the in-service examination requirement. Such the crack integrity assessment is performed by comparing critical crack sizes with end-of-period crack sizes calculated by fatigue analysis.

In ASME B&PV Code Section XI, critical crack sizes are presented only for straight pipes according to piping sizes and loading conditions (KINS, 2009). Thus, it is restrictive to apply the same criteria to various piping types such as elbows, branches and reducers. Especially for branches, there are many variables related to geometries, load directions, and crack locations which may lead to very

different crack behaviours compared to those of straight pipes. Therefore, in order to evaluate the crack integrity of branches, it is necessary to determine the exact critical crack sizes as considering the various parameters using detailed FE analysis.

In this paper, the CCLs of weldolet weldments of T-branches were evaluated using CDFD method (Anderson, 2005) based on FE analyses. In terms of crack locations, the circumferential through-wall cracks (TWCs) were postulated on the upper fusion line. The two locations (crotch and flank sides) along the circumference of weldment were considered. As for loading conditions, combined loads of pressure, bending, and tension corresponding to faulted conditions were considered. The applied *J*-integral curves were plotted as calculating *J* values according to crack length using elastic-plastic FE analyses. Finally, the CCLs were determined by finding the instability point between the weld material *J*-*R* curve and the applied *J*-integral curves.

ELASTIC-PLASTIC FINITE ELEMENT ANALYSIS

Geometry and boundary condition

6″ and 8″ weldolets of main steam pipeline of advanced Korean standard nuclear power plants were considered in the present study. The circumferential TWCs were assumed on the upper fusion line as illustrated in Fig. 1 (a) and (b) where the ultrasonic testing (UT) inspection in the axial direction was not possible. In order to evaluate the crack integrity according to crack locations, the cracks were located at crotch side (0°) and flank side (90°) as shown in Fig. 1 (c). The crack sizes (θ/π) for investigating the *J* versus crack lengths are summarized in Table 1 according to weldolet sizes and crack locations, where θ denotes the half crack angle as defined in Fig. 1 (c).

Table 1. Summary of crack sizes employed in the present FE analyses according to weldolet sizes and crack locations

θ/π	6″	8″
Crotch	0.5, 0.58, 0.62, 0.67	0.15, 0.3, 0.5, 0.55, 0.6
Flank		0.2, 0.35, 0.5, 0.57, 0.65

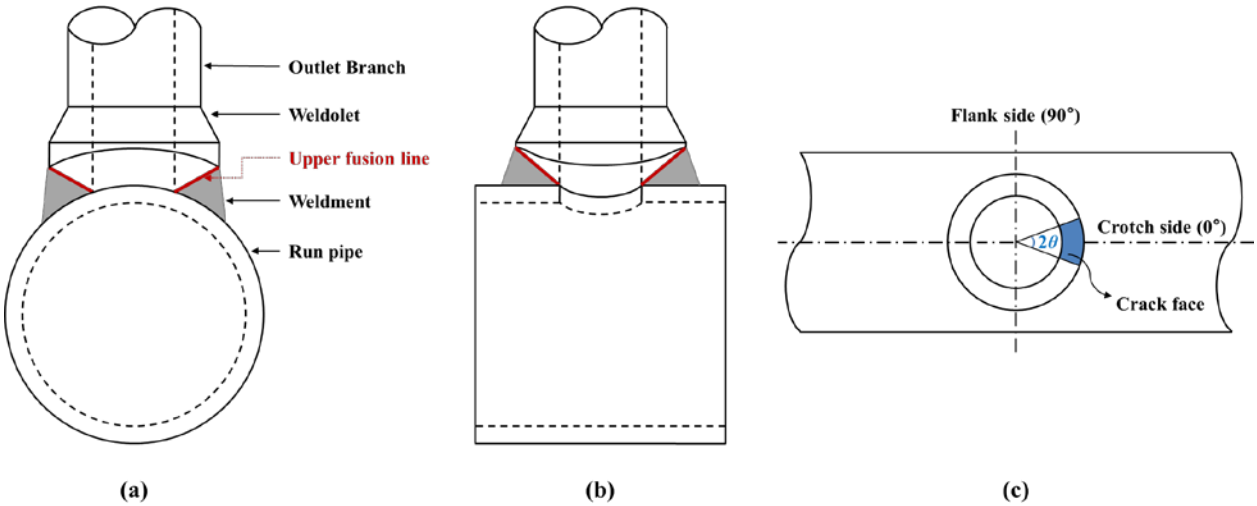

Figure 1. Geometry of a T-branch with weldolet; (a) side view (b) front view (c) crack location and shape at crotch side

Fig. 2 shows the 3-dimensional FE model of 6″ weldolet with circumferential TWC located at crotch side. The half model was adopted as applying symmetry condition for the crotch side crack model, while the full model was used for the flank side crack model to which the out-of-plane bending was applied. In order to avoid incompressibility problems, the iso-parametric brick reduced integration element, C3D20R in Abaqus (2014) element library, was utilized.

As shown in Fig. 3, one of the run pipe ends was fixed, and the combined loads of design internal pressure, tension, and bending were considered, where the tension and bending loads are corresponded to faulted conditions. The distributed load for internal pressure was applied to the inside surface of the pipeline together with the end-cap loads at the end of branch and run pipes. In addition, the half magnitude of the internal pressure to the crack face was employed. For the bending moment, all of the nodes on pipe end were constrained to the single master node located at the centre of pipe end using multi-point constraints (MPC) option within Abaqus (2014). The bending moment was applied to the each master node of pipe ends with consideration of the bending direction inducing maximum crack opening behaviour for each crack location. For the axial tension, the corresponding distributed load was applied to the end of branch and run pipes.

For the elastic-plastic analyses, the material behaviour follows the Ramberg-Osgood (R-O) relation:

$$\frac{\varepsilon}{\varepsilon_y} = \frac{\sigma}{\sigma_y} + \alpha\left(\frac{\sigma}{\sigma_y}\right)^n \tag{1}$$

where, the ε_y and σ_y denote yielding strain and strength, respectively, α is R-O coefficient, n is the strain hardening exponent. The Young's modulus, Poisson's ratio, yield strength, α, and n were set to be E=29,000 ksi, v=0.3, σ_y =26.7 ksi, α=0.969, and n=4.99, respectively, which were determined from lower bound data of the tensile tests (ASTM, 2008) of the base material.

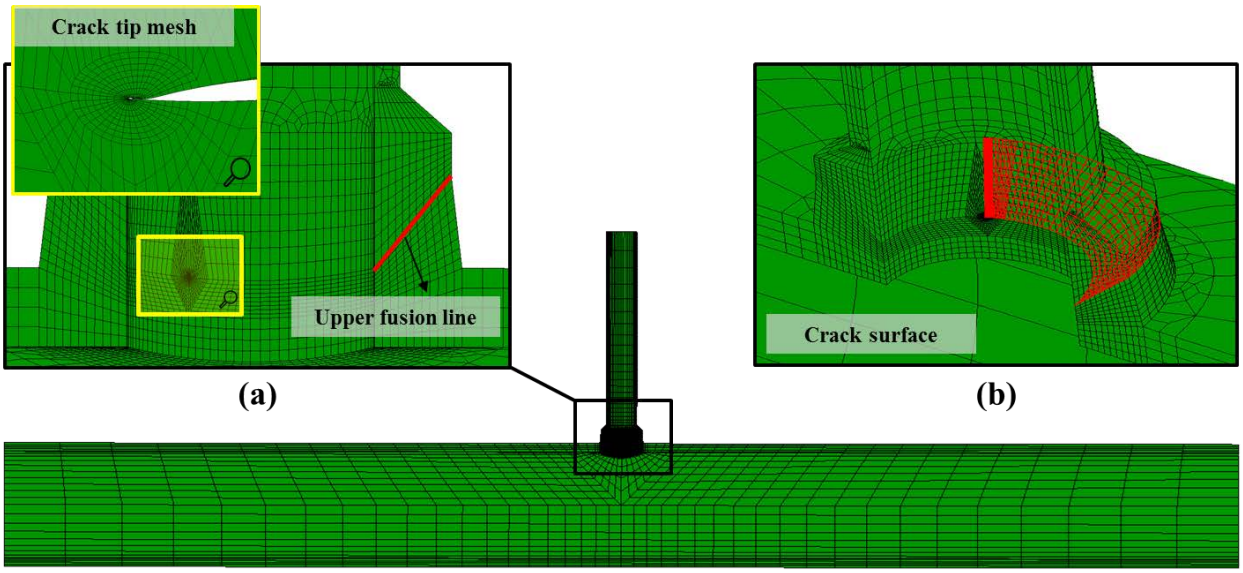

Figure 2. FE model of 6″ branch; (a) weldolet part (b) circumferential TWC located at crotch side

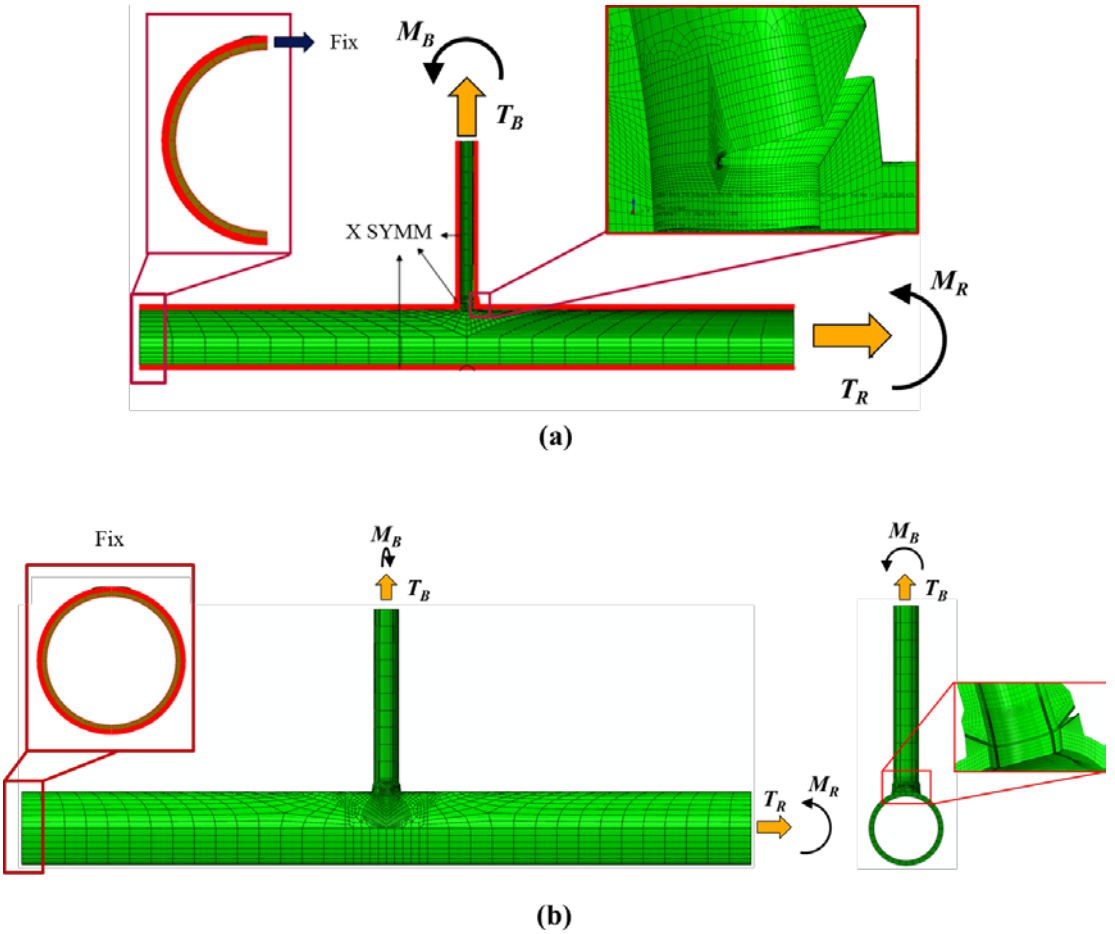

Figure 3. Loading and boundary conditions of (a) crotch side crack model (b) flank side crack model

FE J-integral calculation

The crack tip mesh was modelled using wedge shape collapsed elements with 8 contours. The elastic-plastic *J*-integral was calculated along the crack front using domain integral method, and the averaged *J* values of the 2nd~7th contours which maintain the path-independence of *J*-integral were used in the present study. Fig. 4 shows the verification of the path-independence of *J* according to the contour number at middle point in the thickness direction for the crotch side crack of 8″ weldolet under the faulted condition.

The number of 21 crack tip nodes were located along the thickness direction, and the averaged *J* values extracted from the each node. Fig. 5 shows the averaged *J* values along the thickness direction, where the location of crack tip nodes is represented by the normalized distance (*x*), where the inside surface point is located at *x*=0, and the outside surface point at *x*=1. Generally, the averaged *J* value in the thickness (J_{avg}) is used to assess the ductile fracture, however, maximum values (J_{max}) were additionally considered for a conservative assessment in the present study. In calculating the two types of *J*, the free surface points (at *x*=0, 1) were excluded due to the inaccuracy of *J* values at those points.

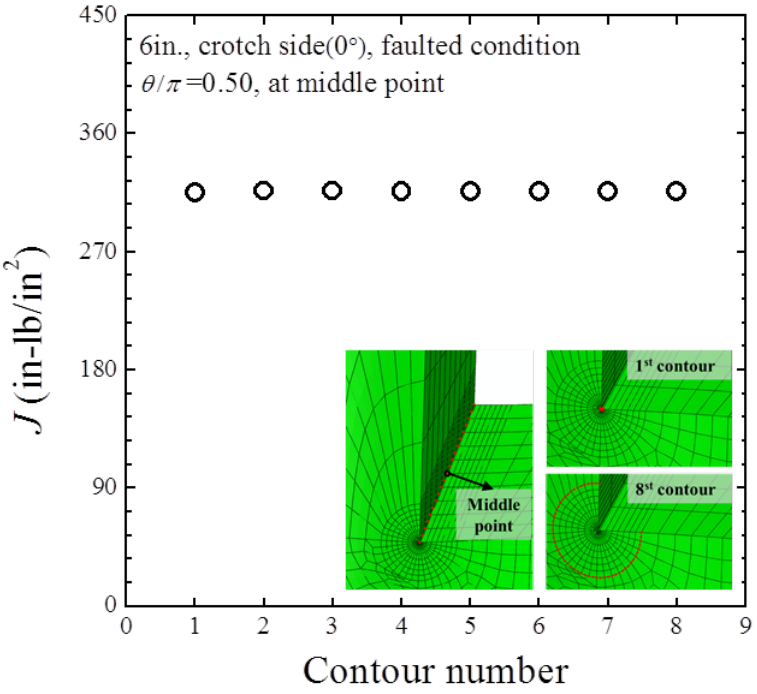

Figure 4. Verification of path-independence of *J* according to contour number

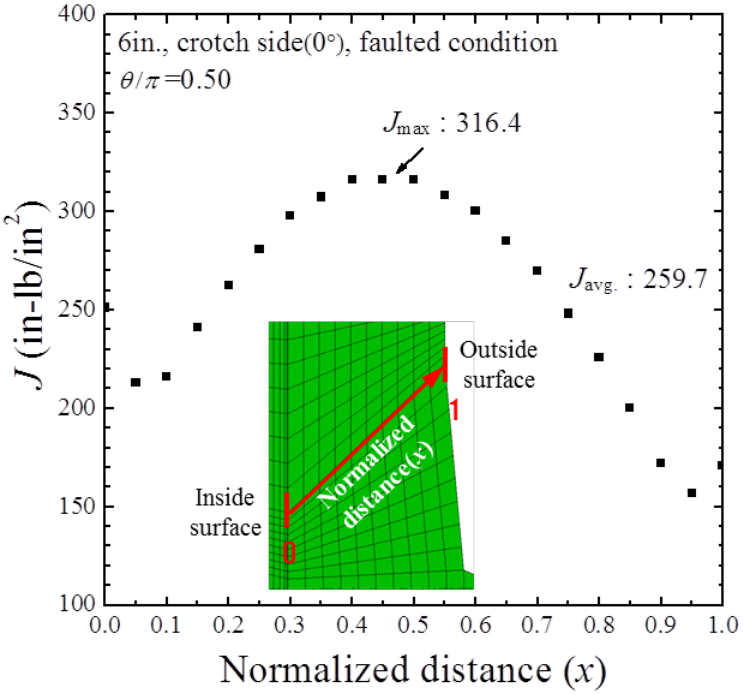

Figure 5. FE *J*-integral results along the thickness for crotch side crack of 6″ weldolet

CRITICAL CRACK LENGTH BASED ON CDFD METHOD

CDFD method

The CDFD method evaluates the crack stability as comparing the crack driving force with fracture toughness of a structure as shown in Fig. 6. The applied J curve can be derived from J values at crack sizes such as a_1~a_5 for a given load, and the J-R curve is shifted along the a-axis to find the tangent instability point. The critical crack size, a_c, is the initial crack size of the J-R curve which meets the applied J curve tangentially. The tangent instability point can be found when the two curves satisfy simultaneously the relations as follows,

$$J_{applied} = J_R \tag{2}$$

$$\frac{dJ_{applied}}{da} = \frac{dJ_R}{da} \tag{3}$$

where, $J_{applied}$ and J_R denote a J value versus crack size of applied J and J-R curves, respectively, and dJ/da expresses the derivative of J curves with respect to crack size.

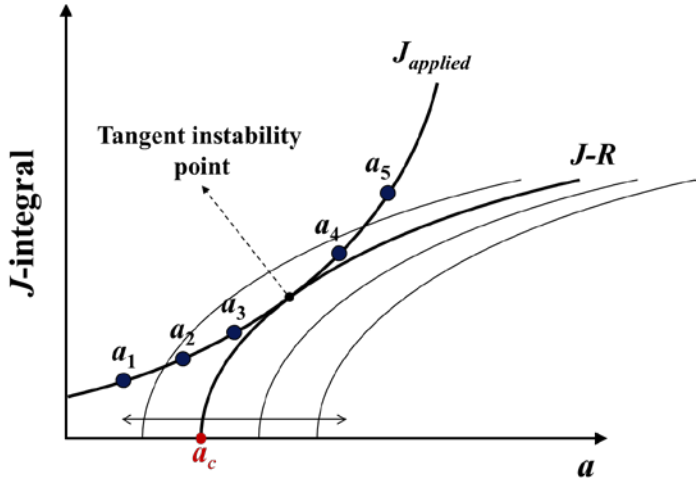

Figure 6. CDFD method for determination of critical crack size

Determination of critical crack length

The applied J curve was fitted to the FE J versus crack length in the form of exponential function as follows,

$$J_{applied}(a) = e^{m_1 + m_2 a + m_3 a^2} \tag{4}$$

where, m_1, m_2, and m_3 denote the constants, a is a crack length.

For the J-R curve, curve-fitting was performed using the power law relation:

$$J_R(a) = C_1\left(\frac{a - a_0}{a^*}\right)^{C_2} \tag{5}$$

where, C_1 and C_2 are the material constants obtained from lower bound data of the *J-R* tests (ASTM, 2003) on weld materials, a^* is 1.0 mm or 0.0394 in. as a conversion factor of unit, a_0 is the initial crack length. The material constants were set to be C_1=1393.0 in-lb/in^2 and C_2=0.333.

Fig. 7 illustrates the CDFD evaluation results for crotch side crack model of 8″ weldolet, and the CCLs are summarized in Table 2 according to the weldolet sizes, crack locations, and types of *J* value (J_{max} or J_{avg}). As expected, the CCLs due to the maximum *J* are shorter than those due to the averaged *J*. According to crack location, there are no significant differences of CCLs. The unstable crack growth would occur when the cracks propagate to about 60% and 50% of the circumference of weldments of 6″ and 8″ weldolets, respectively.

Table 2. Summary of CCLs according to weldolet sizes, crack locations, and types of *J* value

Critical crack length [in.] (% of circumference)	**Crotch**		**Flank**	
	J_{avg}	J_{max}	J_{avg}	J_{max}
6″	6.94 (61.9%)	6.81 (60.7%)	6.84 (61.0%)	6.72 (59.9%)
8″	6.66 (52.5%)	6.53 (51.4%)	6.74 (53.1%)	6.64 (52.3%)

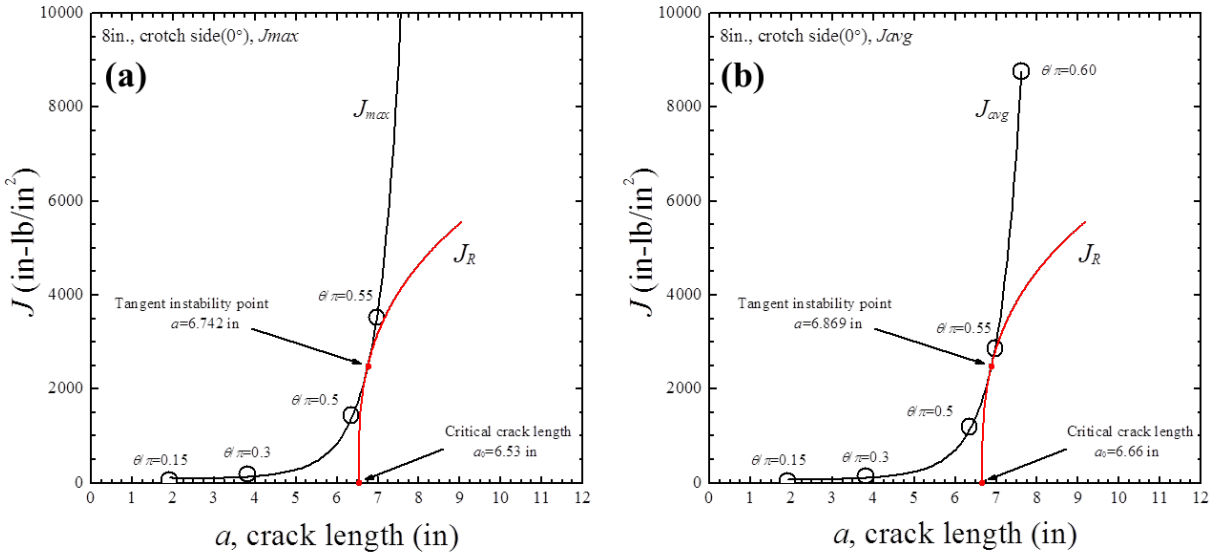

Figure 7. CDFD evaluation results for crotch side crack model of 8″ weldolet based on (a) averaged *J* (b) maximum *J*

CONCLUSION REMARKS

In this study, the CCLs for 6″ and 8″ weldolet weldments of T-Branches with circumferential TWCs were determined using CDFD method based on FE analyses. The crack locations were postulated at crotch and flank sides. As for the loading conditions, the combined loads of design pressure, tension and bending corresponding to faulted conditions were considered. In terms of material properties, the stress-strain behaviour and fracture toughness were obtain from lower bound data of tensile tests of the base material and *J-R* tests of the weld material, respectively. Four or five crack lengths for each crack location were employed for elastic-plastic FE analyses to obtain the *J* trend, and the both averaged and maximum *J* values in the thickness were adopted to plot the applied *J* curves for CDFD evaluation. The CCLs results from CDFD evaluation show that the crack growth would be stable before the TWCs propagate to about 60% of circumference of weldment for 6″ weldolet, and 50% of that for 8″ weldolet. These results are expected to be used for the assessment of piping rupture during operation life in comparison to end-of-period crack sizes.

ACKNOWLEDGEMENTS

This study is supported by the Korea Hydro and Nuclear Power Co., Ltd. as the structural integrity evaluation project on weldolets in pipe break exclusion regions.

REFERENCES

Abaqus User Manual. (2014). Dassault Systemes, Release 6.14.

American Society for Testing Materials. (2003). “E1820 Standard Test Method for Measurement of Fracture Toughness,” *Annual Book of ASTM standards*, USA.

American Society for Testing Materials. (2008). “E8 Standard Test Methods for Tension Testing of Metallic Materials,” *Annual Book of ASTM standards*, USA.

Anderson, T. L. (2005). *Fracture Mechanics; Fundamentals and Applications, 3rd Edition*, CRC Press. USA.

Korea Institute of Nuclear Safety. (2009). *Development of a Flaw Integrity Regulation Code for Primary System Piping*, KINS/RR-706, KOR.

Korea Institute of Nuclear Safety. (2014). *Safety Review Guidelines for Light Water Reactors*, KINS/GE-N001, Revision 4, KOR.

U.S. Nuclear Regulatory Commission. (2016). “Chapter 3.6.2: Determination of Rupture Locations and Dynamic Effects Associated with the Postulated Rupture of Piping, *Standard Review Plan*, USA

U.S. Nuclear Regulatory Commission. (2017). “Inspection Procedure 73054, Part 52: Preservice and Inservice Inspection – Review of Program,” *NRC Inspection Manual*, USA.

Virginia Electric and Power Company. (2005). *Virginia Electric and Power Company Surry Power Station Unit 2 ASME Section XI Inservice Inspection (ISI) Relief Request Main Steam Line Branch Connection Weldolets*, Relief Request SPT-008, Richmond, Virginia, USA.

Virginia Electric and Power Company. (2006). *Virginia Electric and Power Company Surry Power Station Unit 2 ASME Section XI Inservice Inspection Program Relief Request CMP-007 Regenerative and Residual Heat Exchangers*, Relief Request CMP-007, Richmond, Virginia, USA.